Ragi K " Structural, corrosion inhibition, chelation, biological and in silico studies of schiff bases." Thesis. Research and Postgraduate Department of Chemistry, St. Thomas' college (autonomous), University of Calicut, 2020.

CHAPTER 4
CORROSION INHIBITION STUDIES OF SCHIFF BASES IN 1.0 M HCl MEDIUM

Investigations on corrosion inhibition efficiency of the Schiff bases 2,2'-(5,5-dimethylcyclohexane-1,3-diylidene)bis(azanylylidene))diphenol (DMCHDP), N,N'-(5,5-dimethylcyclohexane-1,3-diylidene)dianiline (DMCHDA), 2,2'-(5,5-dimethylcyclo hexane-1,3-diylidene)bis(hydrazinecarboxamide) (DMCHHC), 2-((2hydroxy benzylidene)amino) phenol (2HBAP), 2-(cyclohexylideneamino)phenol (2CHAP) having concentration in the range 0.2-1.0 mM on mild steel were conducted in 1.0 M HCl. Mild steel specimens were prepared as per ASTM standards. Corrosion monitoring techniques employed for the study are gravimetric (weight loss) and electrochemical studies (electrochemical impedance spectroscopy, potentiodynamic polarization studies and electrochemical noise measurements). To illustrate the mechanism of inhibition by Schiff base molecule adsorption studies were also carried out. Thermodynamic parameters of corrosion of mild steel such as activation energy (E_a), enthalpy of activation (ΔH^*), entropy of activation (ΔS^*) and Arrhenius factor (A) were evaluated using temperature dependent gravimetric investigations. Surface morphology of mild steel specimens were also determined using scanning electron microscope. Quantum chemical studies were done to illustrate the efficiency of these Schiff bases as corrosion inhibitor on mild steel in acid medium.

Weight loss studies

Parameters of corrosion such as rate of corrosion and corrosion inhibition efficiency obtained by weight loss studies carried out on mild steel specimens in 1.0 M HCl using Schiff bases (DMCHDP, DMCHDA, DMCHHC, 2HBAP and 2CHAP) at different concentrations for 24 h are shown in Table 4.1 and Table 4.2 respectively. Data

clearly showed that the rate of corrosion decreased with the concentration of Schiff bases in all cases except for 2HBAP. Comparison of corrosion rate of mild steel at different concentrations of the Schiff bases DMCHDP, DMCHDA, DMCHHC, 2HBAP and 2CHAP in 1.0 M HCl are shown in Fig. 4.1.

Table 4.1 Rate of corrosion of MS in mmy^{-1} with and without Schiff bases DMCHDP, DMCHDA, DMCHHC, 2HBAP and 2CHAP in 1.0 M HCl

Conc	Schiff base				
(mM)	DMCHDP	DMCHDA	DMCHHC	2HBAP	2CHAP
0.0	7.304	7.304	7.304	7.304	7.304
0.2	1.207	1.411	1.208	12.134	5.443
0.4	1.088	1.285	1.130	10.827	3.953
0.6	0.523	1.017	0.960	10.385	3.642
0.8	0.464	0.873	0.617	9.075	2.692
1.0	0.437	0.538	0.507	9.074	1.490

Table 4.2 Corrosion inhibition efficiency (η_w%) of Schiff bases DMCHDP, DMCHDA, DMCHHC, 2HBAP and 2CHAP on MS in 1.0 M HCl

Conc	Schiff base				
(mM)	DMCHDP	DMCHDA	DMCHHC	2HBAP	2CHAP
0.2	83.46	80.67	83.45	-66.13	25.47
0.4	85.09	82.39	84.52	-48.23	45.86
0.6	92.83	86.07	86.84	-42.18	50.12
0.8	93.63	88.04	91.54	-24.25	63.14
1.0	94.01	92.63	93.05	-24.23	79.60

The ligands DMCHDP, DMCHDA and DMCHHC have high corrosion inhibition efficiency compared to 2HBAP and 2CHAP. Also the inhibition efficiency of these three ligands is greater than 80% at all studied concentrations. At 1 mM concentration, maximum efficiency of about 94.01%, 92.63% and 93.05% was reached by DMCHDP, DMCHDA and DMCHHC respectively. As the concentration increases, number of molecules required to block the reaction sites also increases. As a result corrosion inhibition efficiency increased with concentration. Comparison of corrosion

inhibition efficiency of the Schiff bases DMCHDP, DMCHDA, DMCHHC, 2HBAP and 2CHAP on MS in 1.0 M HCl are shown in Fig. 4.2.

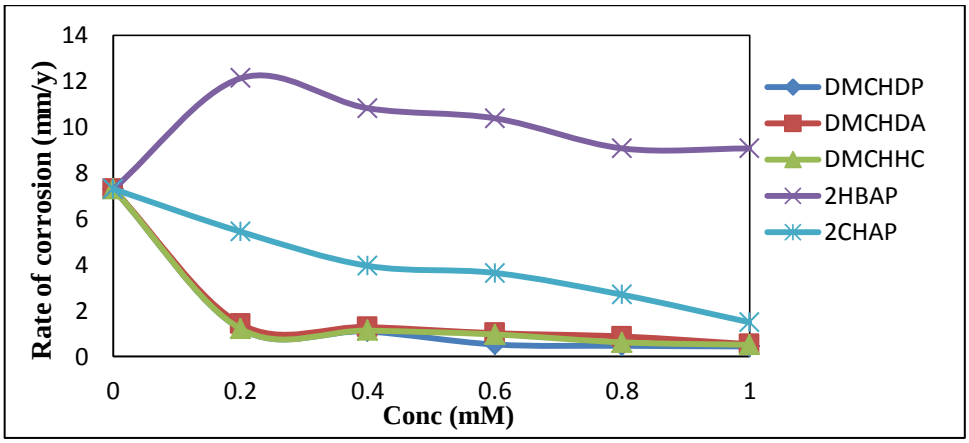

Fig. 4.1 Comparison of corrosion rate of mild steel at different concentrations of the Schiff bases DMCHDP, DMCHDA, DMCHHC, 2HBAP and 2CHAP in 1.0 M HCl

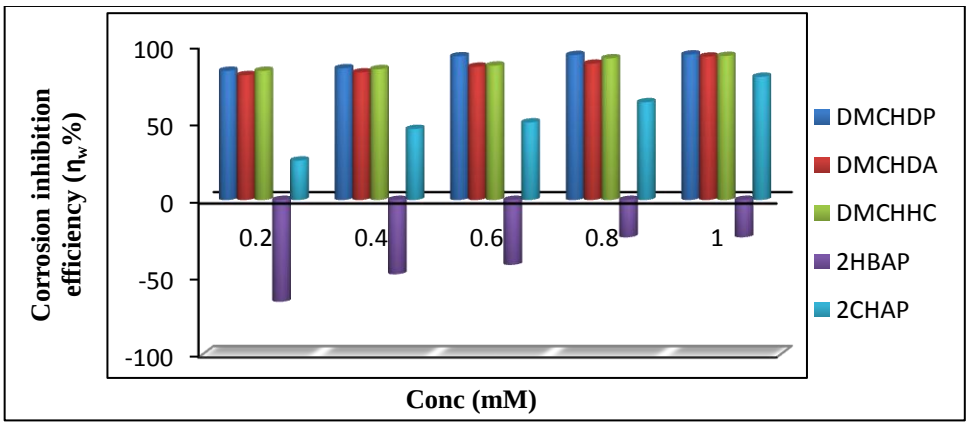

Fig. 4.2 Comparison of corrosion inhibition efficiency (η_w%) of the Schiff bases DMCHDP, DMCHDA, DMCHHC, 2HBAP and 2CHAP on MS in 1.0 M HCl

Presence of azomethine (>C=N-) groups and aromatic rings are responsible for the enhanced activity of DMCHDP and DMCHDA. In addition, the hydroxyl group present in DMCHDP enhanced its efficiency. In DMCHHC azomethine group and hetero atoms such as N and O are responsible for the high inhibition capacity.

But in 2HBAP, even though the rate is decreasing with rise in concentration, it is higher than the blank specimen. As a result 2HBAP exhibits antagonistic nature on corrosion. Antagonistic effect of 2HBAP may be due to any one of the following reasons

or their combined effects: 1) evolution of hydrogen as a result of catalytic action of the compound adsorbed on metal 2) decrease of overpotential for cathodic processes 3) formed complex is easily soluble and it lowered the overpotential for cathodic processes.

Comparison between η_w% of Schiff bases with its parent compounds

In order to compare the corrosion inhibition efficiency of the Schiff bases with the corresponding aldehydes/ketones and amines from which they synthesized, weight loss measurement of the parent compounds were also conducted at concentrations 0.2 mM, 0.6 mM and 1.0 mM. The aldehyde, ketone and amines used for the synthesis are salicylaldehyde (SAY), 5,5-dimethyl-1,3-cyclohexanedione (DM), cyclohexanone (CH), 2-aminophenol (2AP), aniline (AN) and semicarbazide (SZ). Results are shown in Table 4.3. Comparison of corrosion inhibition efficiency of parent compounds and Schiff bases on MS in 1.0 M HCl are shown in Fig. 4.3.

Table 4.3 Corrosion inhibition efficiency (η_w%) of Schiff bases and their parent compounds on MS in 1.0 M HCl

Compounds	Conc (mM)		
	0.2	0.6	1.0
DM	-85.40	-70.67	-42.56
2AP	-98.50	-67.76	-65.68
AN	-70.19	-8.46	25.70
SZ	-140.38	-133.79	-133.56
SAY	-111.73	-80.13	-60.47
CH	-136.78	-130.44	-109.77
DMCHDP	83.46	92.83	94.01
DMCHDA	80.67	86.07	92.63
DMCHHC	83.45	86.84	93.05
2HBAP	-66.13	-42.18	-24.23
2CHAP	25.47	50.12	79.60

From the table it is clear that the parent compounds have antagonistic effect on corrosion and inhibition efficiency of all the Schiff bases is remarkably higher than the

parent compounds. This is due to the participation of electron rich >C=N- group present in the Schiff base ligands in the corrosion inhibition process.

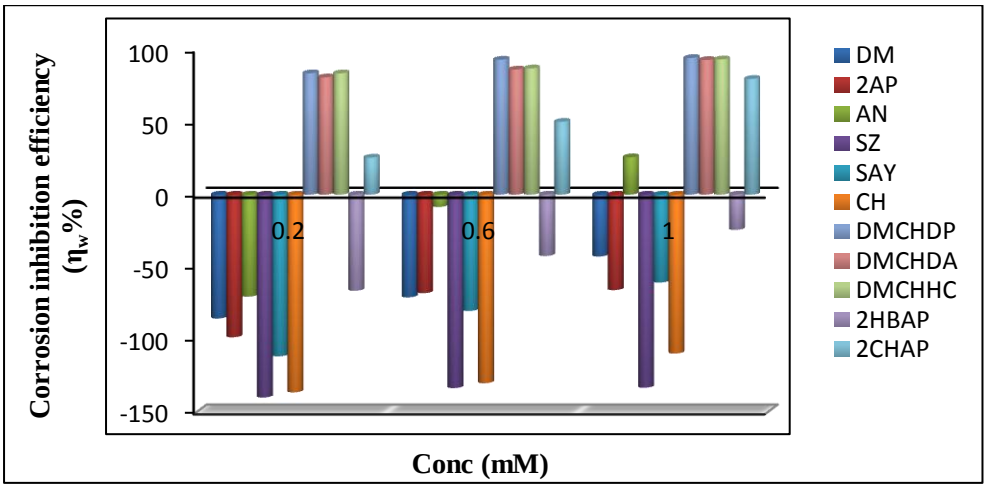

Fig. 4.3 Comparison of corrosion inhibition efficiency (η_w%) of Schiff bases and their parent compounds on MS in 1.0 M HCl

Adsorption studies

Adsorption isotherms are useful to elucidate information regarding structural and thermodynamic parameters of the electrical double layer. Corrosion inhibition property of the organic compounds on MS surface is mainly due to adsorption. Therefore it is essential to understand the mode of adsorption that gives information regarding interaction of inhibitor molecule and MS surface. For this purpose different isotherms such as Langmuir, El-Awady, Frumkin, Temkin, Freundlich, and Florry-huggin isotherms were plotted and the best fit one was identified using correlation coefficient (R^2). Correlation coefficients obtained for the Schiff bases in various isotherms are given in Table 4.4.

Thermodynamic parameters obtained from the study are free energy of adsorption (ΔG^0_{ads}) and adsorption equilibrium constant (K_{ads}). Adsorption study clearly showed that the three Schiff bases DMCHDP, DMCHDA and DMCHHC were found to obey Langmuir adsorption isotherm whereas 2HBAP and 2CHAP obeyed Frumkin adsorption isotherm on MS surface in 1.0 M HCl medium.

Table 4.4 Correlation coefficients of the Schiff bases derived from various adsorption isotherms

Isotherm	Correlation coefficient (R^2)				
	DMCHDP	DMCHDA	DMCHHC	2HBAP	2CHAP
Langmiur	0.9988	0.9969	0.9979	0.9299	0.8522
Freunlich	0.8540	0.9762	0.9534	0.9066	0.9684
Frumkin	0.9541	0.9634	0.9421	0.9450	0.9756
Temkin	0.8522	0.8553	0.8221	0.9007	0.9331
El-Awady	0.8725	0.7968	0.8021	0.8996	0.9185
Florry Huggin	0.8479	0.7552	0.7695	0.7241	0.6145

Thermodynamic parameters obtained from the analysis of isotherms are given in Table 4.5 and the adsorption isotherms of Schiff base molecules on MS surface in 1.0 M HCl medium are described in Fig. 4.4.

Table 4.5 Thermodynamic parameters for the adsorption of DMCHDP, DMCHDA, DMCHHC, 2HBAP and 2CHAP on MS in 1.0 M HCl

Parameter	Schiff base				
	DMCHDP	DMCHDA	DMCHHC	2HBAP	2CHAP
Correlation coefficient (R^2)	0.9988	0.9969	0.9979	0.9450	0.9756
K_{ads}	20000	16666.66	20000	3333.33	2385.61
ΔG^0_{ads} ($kJmol^{-1}$)	-34.86	-34.40	-34.86	-30.37	-29.53

The ΔG^0_{ads} values upto -20 $kJmol^{-1}$ indicate that the interaction of charged molecule and charged metal surface is electrostatic in nature (physisorption) while if its value is more negative than -40 $kJmol^{-1}$ indicates the presence of co-ordinate type bond between Schiff base molecules and metal surface (chemisorption). Negative values of ΔG^0_{ads} in all case indicate spontaneity of the process. In the case of Schiff bases subjected to adsorption studies the ΔG^0_{ads} values varies from -29.53 $kJmol^{-1}$ to -34.86 $kJmol^{-1}$. This indicates that the adsorption behaviour of all Schiff bases involves both electrostatic and chemical interaction. High value of adsorption equilibrium constant (K_{ads}) of DMCHDP, DMCHDA and DMCHHC than the other two Schiff base ligands indicates strong interaction of them on MS surface.

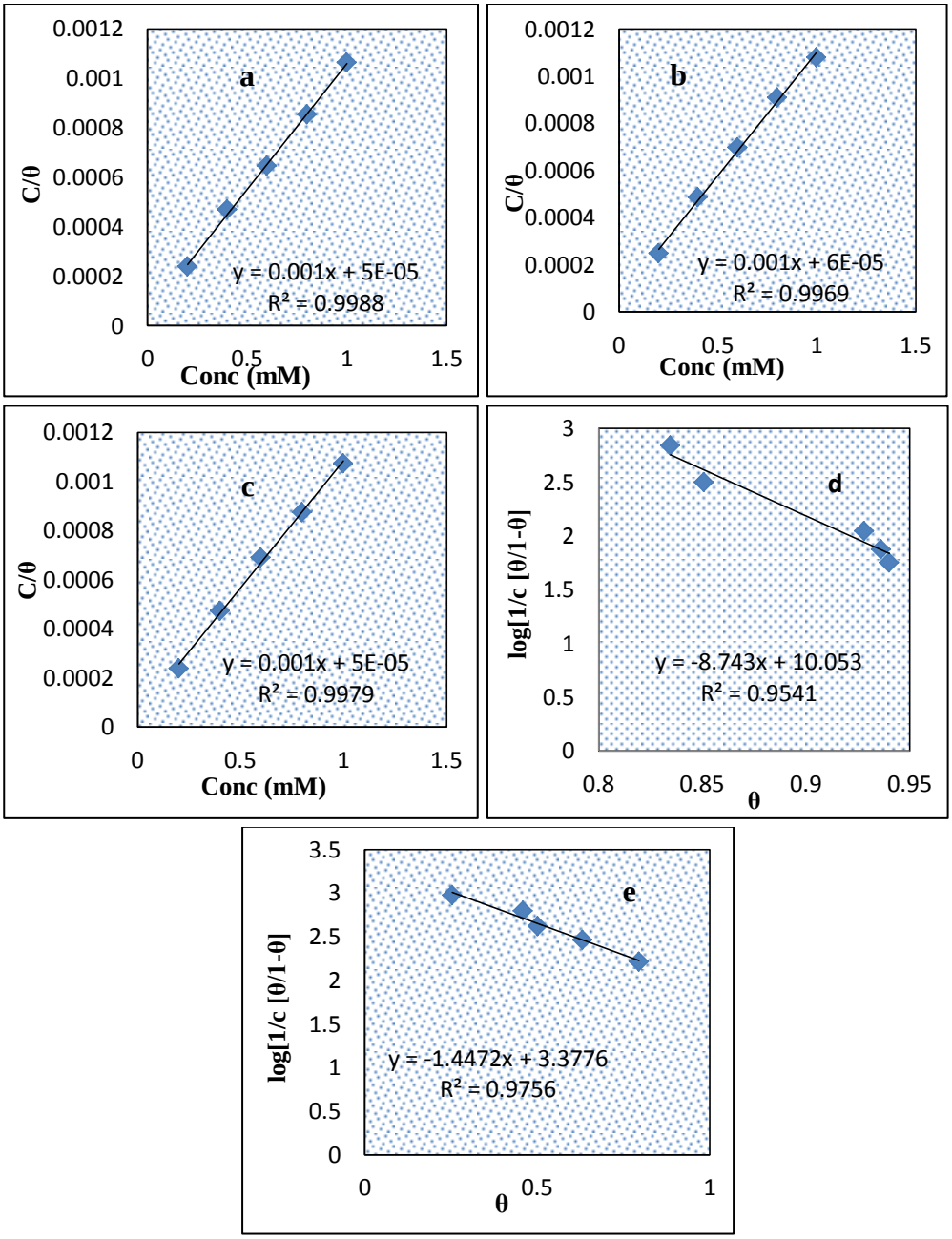

Fig. 4.4 Langmuir adsorption isotherm of a) DMCHDP b) DMCHDA and c) DMCHHC and Frumkin adsorption isotherm of d) 2HBAP and e) 2CHAP on MS in 1.0 M HCl at 28^0C

Temparature studies

Temperature dependent gravimetric investigations definitely benchmark the mode of corrosion inhibition process. Degree of corrosion is dependent on temperature, remarkably in acid media associated with hydrogen evolution. In the present work, the impact of temperature on the inhibition process was investigated using weight loss

studies for 24 h in 1.0 M HCl with and without Schiff bases (DMCHDP, DMCHDA, DMCHHC, 2HBAP and 2CHAP) at temperatures 301 K, 313 K, 323 K and 333 K.

Activation energy of metal dissolution was measured using an Arrhenius type equation given below

$$K = A\exp(-E_a/RT) \quad (1)$$

where K, A, E_a, R and T represents corrosion rate, pre-exponential factor, activation energy, universal gas constant, temperature in Kelvin respectively.

Straight lines obtained by plotting log K vs 1/T for MS specimens in acid, with and without Schiff bases are shown in Fig. 4.5- 4.9a.

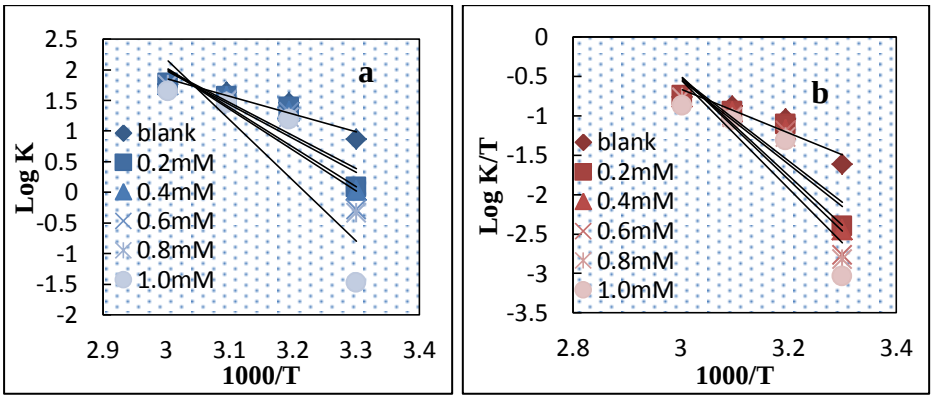

Fig.4.5 Plot of a) log K vs 1000/T b) log K/T vs 1000/T with and without DMCHDP on MS in 1.0 M HCl

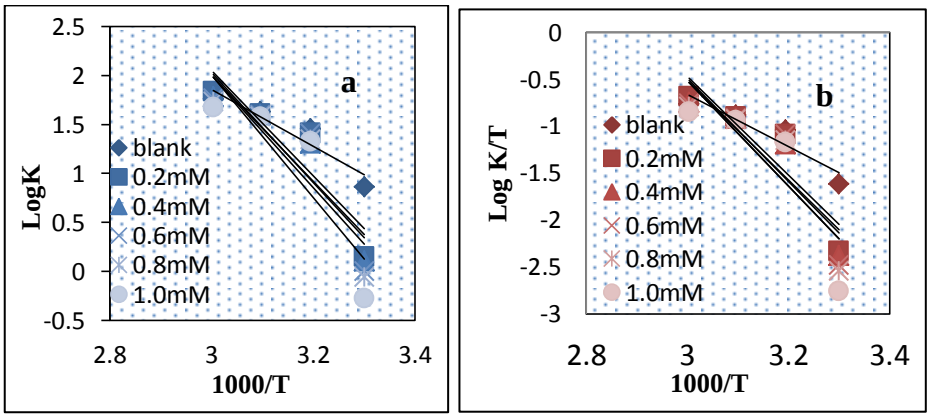

Fig. 4.6 Plot of a) log K vs 1000/T b) log K/T vs 1000/T with and without DMCHDA on MS in 1.0 M HCl

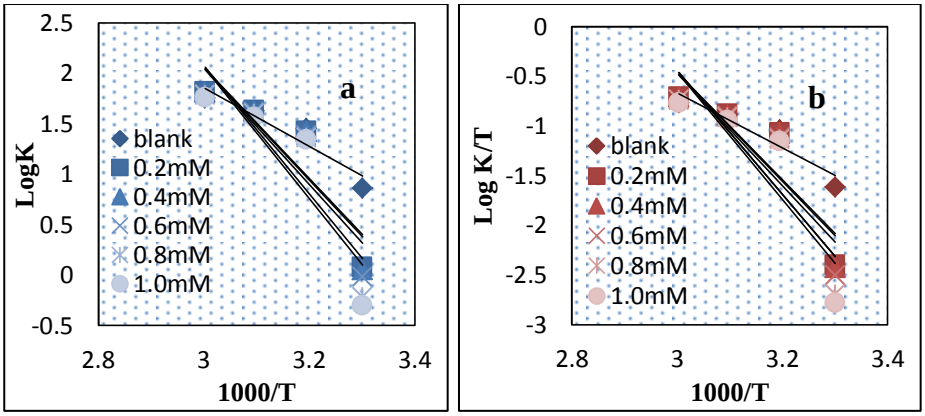

Fig. 4.7 Plot of a) log K vs 1000/T b) log K/T vs 1000/T with and without DMCHHC on MS in 1.0 M HCl

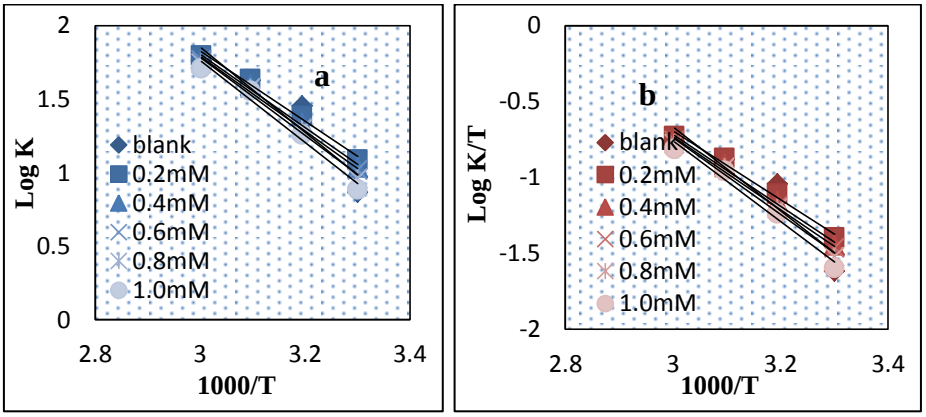

Fig. 4.8 Plot of a) log K vs 1000/T b) log K/T vs 1000/T with and without 2HBAP on MS in 1.0 M HCl

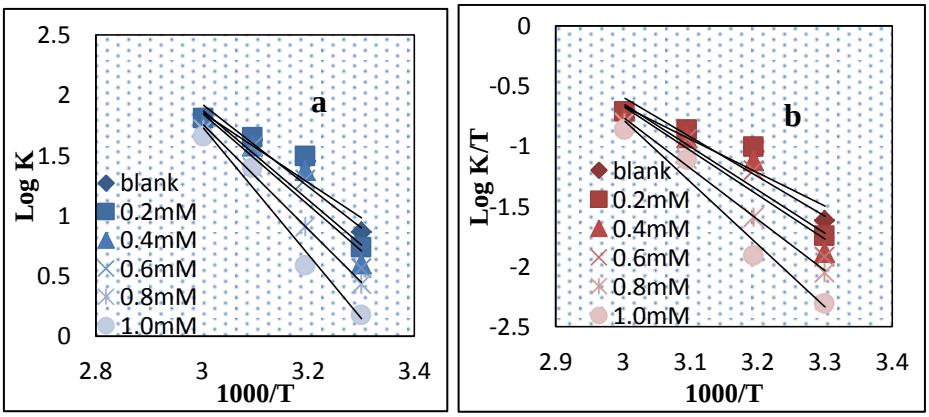

Fig. 4.9 Plot of a) log K vs 1000/T b) log K/T vs 1000/T with and without 2CHAP on MS in 1.0 M HCl

Activation energy needed for the metal dissolution in 1.0 M HCl was obtained from the slope of these plots. Thermodynamic parameters such as enthalpy (ΔH^*) and entropy (ΔS^*) were evaluated using transition state theory (equation 2).

$$K = \left(\frac{RT}{Nh}\right) \exp\left(\frac{\Delta S^*}{R}\right) \exp\left(\frac{-\Delta H^*}{RT}\right) \quad (2)$$

where N is the Avogadro number and h is the Planck's constant. Value of ΔH^* was obtained from the slope $(\frac{-\Delta H^*}{2.303R})$ whereas the value of ΔS^* was obtained from the intercept $(\log(\frac{R}{2.303Nh}) + (\frac{\Delta S^*}{2.303R}))$ of the plot between log K/T vs 1/T for the metal dissolution in 1.0 M HCl (see Fig. 4.5- 4.9b). The values of parameters such as activation energy (E_a), Arrhenius factor (A), enthalpy of activation (ΔH^*) and entropy of activation (ΔS^*) are given in Table 4.6

Table 4.6 Thermodynamic parameters of corrosion of MS with and without Schiff bases in 1.0 M HCl

Schiff base	Conc (mM)	E_a (kJ mol^{-1})	A	ΔH^* (kJ mol^{-1})	ΔS^* (J mol^{-1}K^{-1})
DMCHDP	Blank	55.67	3.81×10^{10}	53.03	-44.26
	0.2	103.04	1.40×10^{18}	100.40	100.59
	0.4	105.58	3.38×10^{18}	102.94	107.92
	0.6	123.53	2.43×10^{21}	120.89	162.60
	0.8	127.55	1.01×10^{22}	124.91	174.49
	1.0	134.58	1.16×10^{23}	131.94	194.77
DMCHDA	0.2	102.76	1.41×10^{18}	100.12	100.64
	0.4	103.55	1.68×10^{18}	100.91	102.10
	0.6	107.13	6.44×10^{18}	104.48	113.26
	0.8	109.73	1.56×10^{19}	107.09	120.65
	1.0	119.48	5.24×10^{20}	116.83	149.65
DMCHHC	0.2	105.97	4.63×10^{18}	103.39	110.54
	0.4	107.16	7.06×10^{18}	104.52	114.05
	0.6	110.70	2.49×10^{19}	108.06	124.54
	0.8	122.27	1.74×10^{21}	119.63	159.85
	1.0	125.31	4.99×10^{21}	122.67	168.58
2HBAP	0.2	45.92	1.06×10^{9}	43.28	-74.05
	0.4	47.86	2.03×10^{9}	45.23	-68.66
	0.6	48.64	2.59×10^{9}	46.00	-66.61
	0.8	51.00	6.00×10^{9}	48.36	-59.64
	1.0	53.57	1.44×10^{9}	50.09	-52.35
2CHAP	0.2	65.71	1.68×10^{12}	63.08	-12.76
	0.4	71.32	1.13×10^{13}	68.68	3.03
	0.6	73.06	2.00×10^{13}	70.42	7.82
	0.8	84.06	8.63×10^{14}	81.43	39.12
	1.0	101.81	4.97×10^{17}	99.18	91.97

It was observed that the activation energy of corrosion in the presence of Schiff bases was higher, compared to metal dissolution without Schiff bases in 1.0 M HCl. Endothermic character of metal dissolution process was reflected from the positive sign of enthalpy. It is also observed that ΔH^* and ΔS^* increased with rise in concentration of inhibitors. Activation energy and enthalpy of corrosion is high in the case of DMCHDP, DMCHDA and DMCHHC compared to 2HBAP and 2CHAP. High corrosion inhibition efficiency of the Schiff bases DMCHDP, DMCHDA and DMCHHC is supported by this observation. Randomness of activated complex goes up with rise in concentration of Schiff bases and ΔS^* acquired positive values.

Electrochemical impedance spectroscopy

The nature of corrosion inhibition of Schiff bases on MS in 1.0 M HCl was evaluated using electrochemical impedance spectroscopy at 28^0C. Impedance spectra (Nyquist and Bode plots) of MS in the absence and presence of Schiff bases at various concentrations in 1.0 M HCl are shown in Fig. 4.10, 4.11, 4.12, 4.13 and 4.14.

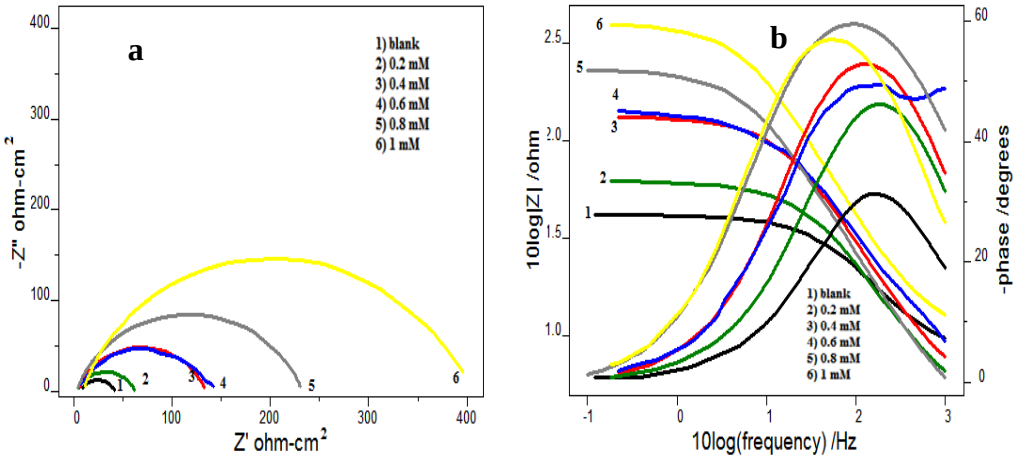

Fig. 4.10 a) Nyquist and b) Bode plots of MS coupons with and without DMCHDP in 1.0 M HCl

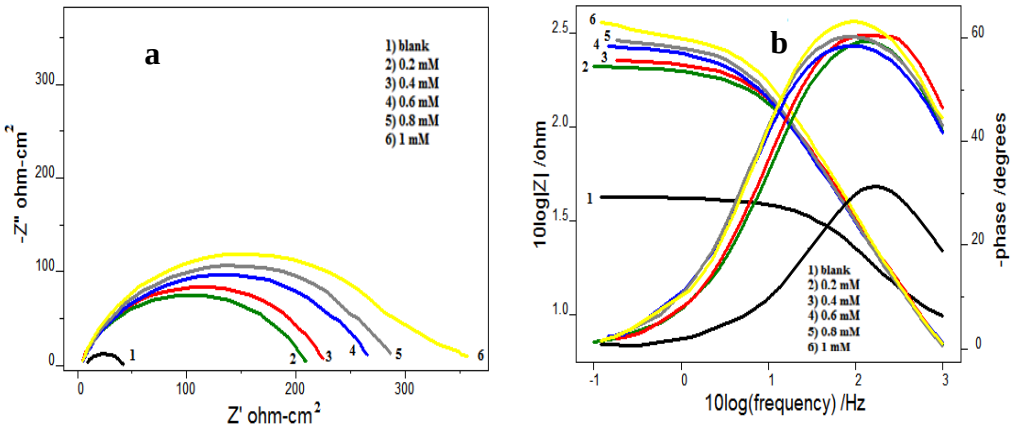

Fig. 4.11 a) Nyquist and b) Bode plots of MS coupons with and without DMCHDA in 1.0 M HCl

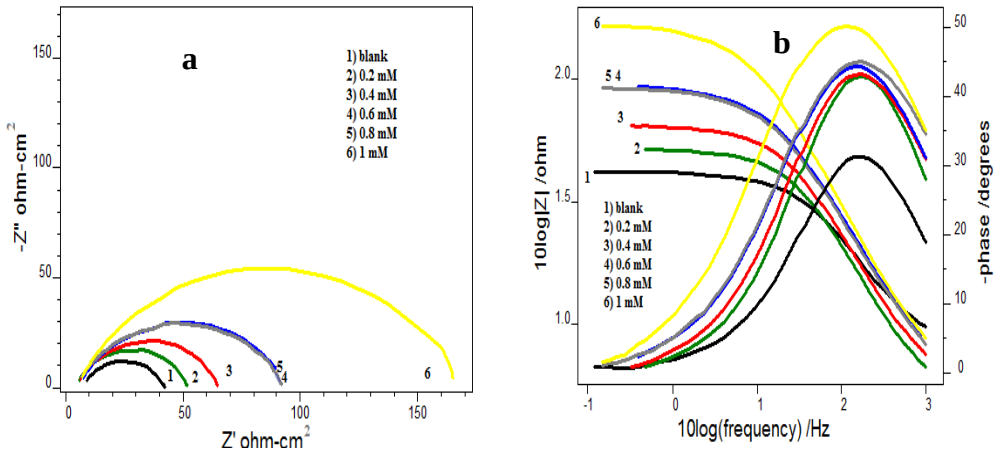

Fig. 4.12 a) Nyquist and b) Bode plots of MS coupons with and without DMCHHC in 1.0 M HCl

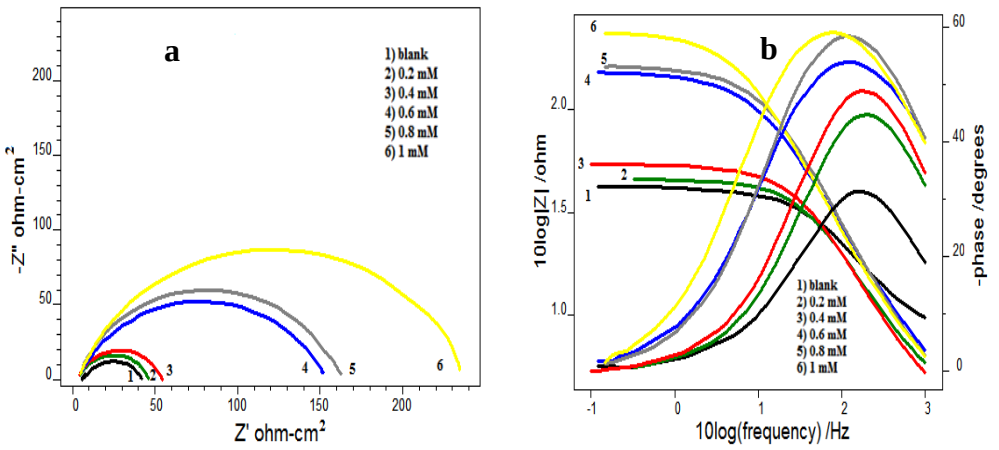

Fig. 4.13 a) Nyquist and b) Bode plots of MS coupons with and without 2HBAP in 1.0 M HCl

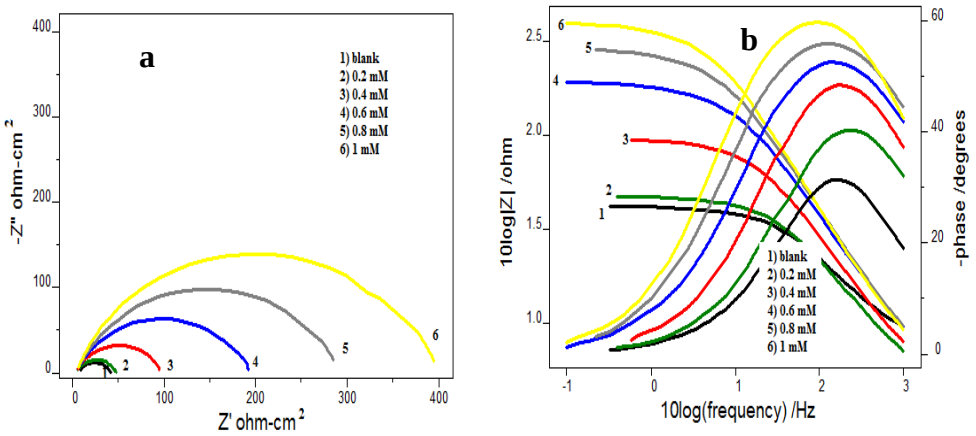

Fig. 4.14 a) Nyquist and b) Bode plots of MS coupons with and without 2CHAP in 1.0 M HCl

Impedance spectra showed a significant change on addition of Schiff bases at various concentrations. Nyquist plots of blank and treated specimen with Schiff bases have similar shape but different size. This indicates that the mechanism of dissolution of metal is same in both cases. Size of the Nyquist plots was found to be increased with rise in concentration of Schiff bases, which indicates that the impedance of MS increased when the concentration increased.

Equivalent circuit used to fit the Nyquist plots (Randles circuit) is shown in Fig. 4.15. The circuit consist of a double layer capacitance C_{dl}, solution resistance R_s and charge transfer resistance R_{ct}. Constant phase element (CPE) is inserted into the circuit in preference to pure double layer capacitance to lower the effects due to deformities on the surface of metal as shown in Fig. 4.15. The impedance of CPE can be expressed as

$$Z_{CPE} = \frac{1}{Y_0(j\omega)^n} \qquad (3)$$

where Y_0 is the magnitude of CPE, n is the exponent (phase shift), w is the angular frequency and j is the imaginary unit. Based on the values of n, CPE can be capacitance, inductance and resistance. It is observed that the values of n is between 0.75 and 1.0, and indicates the nature of capacitance of CPE. Impedance data such as R_{ct}, C_{dl} and the percentage of inhibition efficiency (η_{EIS}%) of the Schiff bases are listed in Table 4.7.

Table 4.7 Impedance data of MS coupons with and without Schiff bases in 1.0 M HCl

Schiff base	Conc (mM)	C_{dl} (μFcm^{-2})	R_{ct} (Ωcm^2)	η_{EIS}%
Blank	0.0	105	29.1	-
DMCHDP	0.2	97.7	50.5	42.37
	0.4	82.8	114	74.47
	0.6	82.0	117	75.12
	0.8	112	202	85.59
	1.0	64.6	349	91.66
DMCHDA	0.2	81.8	181	83.92
	0.4	81.6	200	85.45
	0.6	99.4	232	87.45
	0.8	92.9	253	88.49
	1.0	65.4	308	90.55
DMCHHC	0.2	104	40.6	28.32
	0.4	103	50.9	42.83
	0.6	99.5	72.8	60.03
	0.8	105	73.2	60.24
	1.0	103	136	85.95
2HBAP	0.2	102	37.4	22.19
	0.4	106	45.2	35.62
	0.6	109	77.62	77.62
	0.8	88.8	79.2	79.21
	1.0	118	86.1	86.08
2CHAP	0.2	96.6	36.2	19.61
	0.4	81.4	76.6	62.01
	0.6	78.3	158	81.58
	0.8	75.8	241	87.92
	1.0	75.8	338	91.39

On observing the results charge transfer resistance (R_{ct}) was found to be increased with concentration whereas capacitance (C_{dl}) value is reduced in the case of all Schiff bases. Charge transfer resistance has an inverse relationship with corrosion rate and is a measure of transfer of electrons across exposed metal surface. Decrease in C_{dl} values is due to the lowering of local dielectric constant and/or increase in thickness of electrical double layer. Corrosion inhibition efficiency (η_{EIS}%) is also found to be increased with concentration. In contradiction to weight loss studies, all the Schiff bases are good inhibitors of corrosion according to impedance measurement. Antagonistic effect on corrosion is exhibited by 2HBAP in weight loss studies. Impedance studies showed that

2HBAP has appreciable corrosion inhibition efficiency. This may be due to the less immersion time in the case of electrochemical studies (30 min) compared to weight loss studies (24 h). Factors such as catalytic action of the adsorbed compound and lowering of overpotential which leads to the antagonistic nature of 2HBAP may predominate only after the time taken for electrochemical analysis.

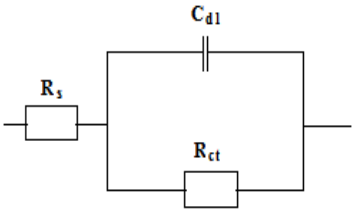

Fig. 4.15 The equivalent circuit used to fit the Nyquist plots

Maximum inhibition efficiency of about 91.66%, 90.55%, 85.95%, 86.08% and 91.39% was exhibited by the Schiff bases DMCHDP, DMCHDA, DMCHHC, 2HBAP and 2CHAP respectively at 1 mM concentration. Comparison of corrosion inhibition efficiency (η_{EIS}%) of the Schiff bases on MS in 1.0 M HCl was shown in Fig. 4.16.

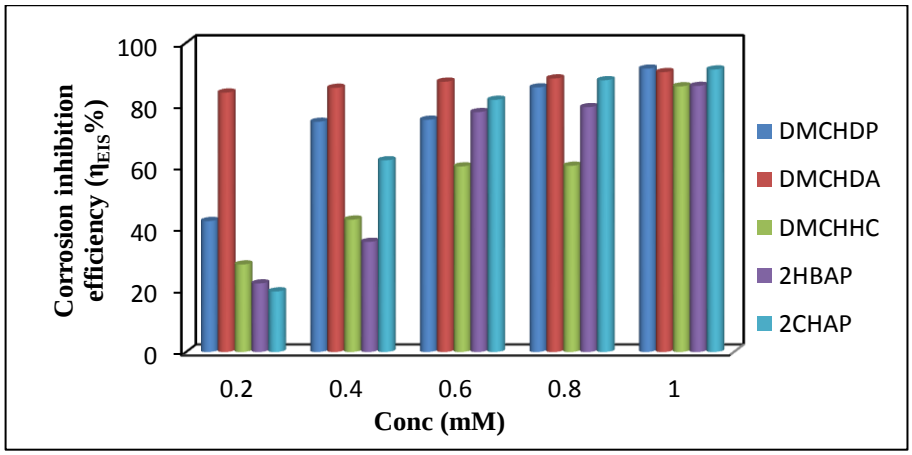

Fig. 4.16 Comparison of corrosion inhibition efficiency (η_{EIS}%) of the Schiff bases on MS in 1.0 M HCl

Potentiodynamic polarization studies

Corrosion inhibition efficiency was also monitored using potentiodynamic polarization studies. This method mainly deals with measurement of current generated as a function of potential or time by varying the potential of working electrode. Two types of polarization techniques such as Tafel and linear polarization were employed for this

purpose. Corrosion current density (I_{corr}) and polarization resistance (R_p) were the main parameters obtained from Tafel and linear polarization techniques respectively. The Tafel and linear polarization plots of the Schiff bases are shown in Fig. 4.17, 4.18, 4.19, 4.20 and 4.21. Polarization data such as corrosion potential (E_{corr}), corrosion current density (I_{corr}), cathodic slope (b_c), anodic slope (b_a), polarization resistance (R_p) and inhibition efficiencies (η_{pol}% and η_{Rp}%) of the Schiff bases in 1.0 M HCl are given in Table 4.8.

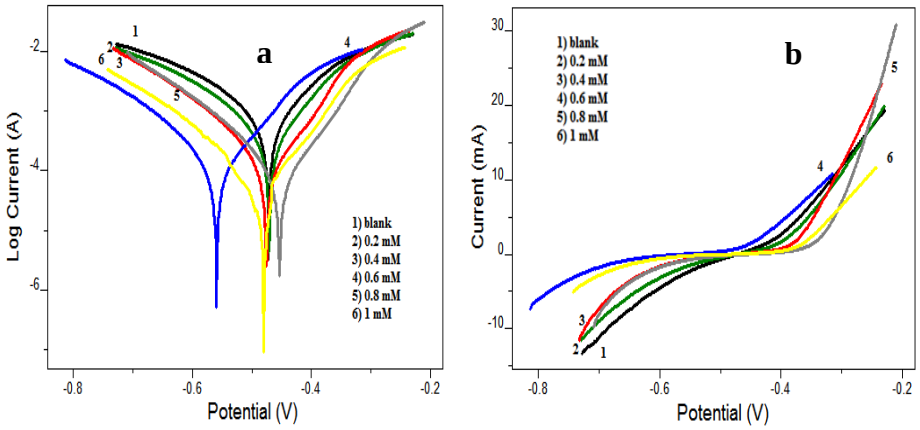

Fig. 4.17 a) Tafel and b) linear polarization plots of MS coupons with and without DMCHDP in 1.0 M HCl

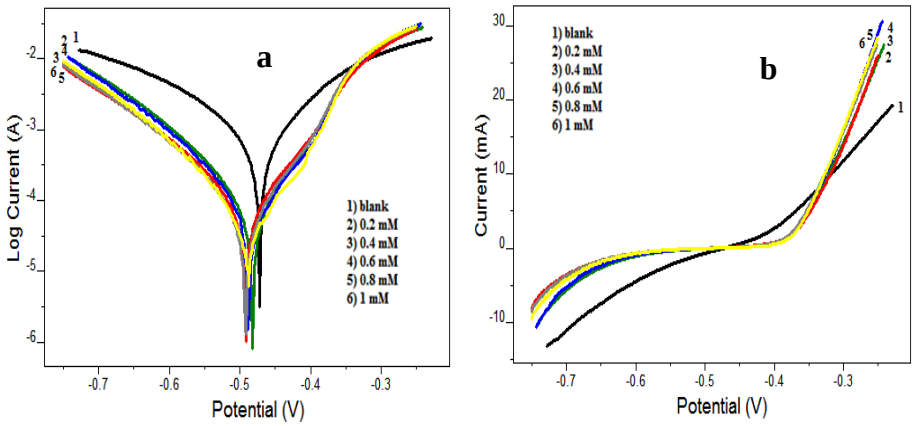

Fig.4.18 a) Tafel and b) linear polarization plots of MS coupons with and without DMCHDA in 1.0 M HCl

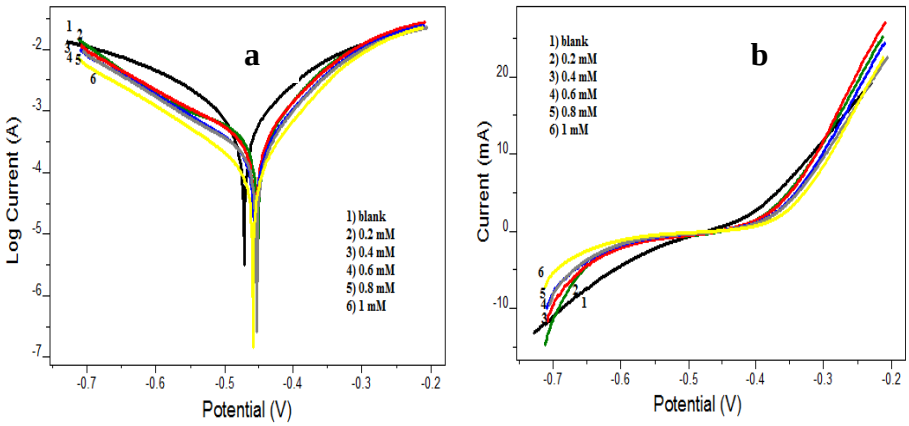

Fig. 4.19 a) Tafel and b) linear polarization plots of MS coupons with and without DMCHHC in 1.0 M HCl

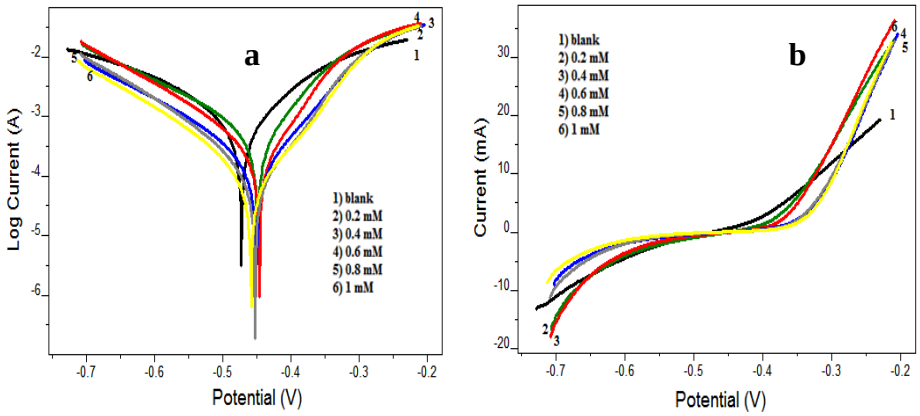

Fig. 4.20 a) Tafel and b) linear polarization plots of MS coupons with and without 2HBAP in 1.0 M HCl

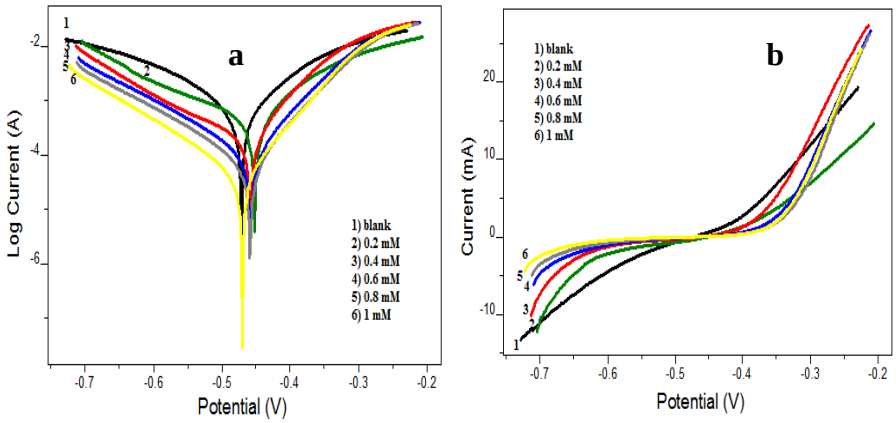

Fig. 4.21 a) Tafel and b) linear polarization plots of MS coupons with and without 2CHAP in 1.0 M HCl

Table 4.8 Polarization data of MS coupons with and without Schiff bases in 1.0 M HCl

Schiff base	Tafel data					Polarization data		
	Conc (mM)	E_{corr} (mV)	I_{corr} (μA/cm2)	b_a (mV/dec)	$-b_c$ (mV/dec)	η_{pol}%	R_p (Ω)	η_{Rp}%
Blank	0.0	-477.3	1160	172	212	-	35.58	-
DMCHDP	0.2	-473.5	640	138	185	44.82	53.56	33.57
	0.4	-461.4	172	83	141	85.21	132.8	73.21
	0.6	-547.2	163	104	150	85.97	187.6	81.03
	0.8	-432.2	98.9	73	135	91.47	207.6	82.86
	1.0	-471.5	59.5	79	130	94.87	360	90.12
DMCHDA	0.2	-468.8	101	73	128	91.31	201.1	82.31
	0.4	-468.9	84.3	71	139	92.73	241.4	85.26
	0.6	-461.1	74	63	126	93.62	247.8	85.64
	0.8	-469.5	67.4	65	129	94.19	278.6	87.23
	1.0	-461.9	51.1	59	121	95.59	335.3	89.39
DMCHHC	0.2	-502.1	461	145	156	60.26	70.82	49.76
	0.4	-454.9	442	133	161	61.89	71.53	50.26
	0.6	-487.4	319	125	148	72.50	92.48	61.53
	0.8	-494.1	309	132	142	73.36	96.26	63.04
	1.0	-458.3	174	108	143	85.00	153.2	76.77
2HBAP	0.2	-469.1	767	134	179	33.88	43.34	17.9
	0.4	-464.4	444	110	149	61.72	61.77	42.39
	0.6	-441.2	193	87	156	83.36	125.6	71.67
	0.8	-442	128	77	132	88.96	165.8	78.54
	1.0	-435	93.3	70	139	91.95	215.7	83.5
2CHAP	0.2	-494.4	605	185	183	47.84	66.18	46.24
	0.4	-504.3	281	123	144	75.77	102.7	65.35
	0.6	-468.8	132	92	147	88.62	187.0	80.97
	0.8	-461.7	83.6	83	146	92.79	275.4	87.08
	1.0	-468.7	46.4	74	133	96.00	444.1	91.99

From the polarization data it is evident that corrosion current density decreased and polarization resistance increased with the concentration of Schiff bases. As a result percentage of corrosion inhibition efficiency was increased. Metal dissolution will be hindered by the adsorbed molecules by inhibiting the anodic or/and cathodic processes of corrosion. On evaluating polarization plots, there is a considerable difference in the slope

of the Tafel lines both in the presence and absence of Schiff base molecules. All the Schiff bases were found to affect both anodic and cathodic sites of corrosion and hence act as mixed type inhibitors. Tafel data revealed that all Schiff bases are good inhibitors of corrosion and the results are in good agreement with that of impedance data. Comparison of corrosion inhibition efficiency (η_{pol}%) of the Schiff bases on MS in 1.0 M HCl is shown in Fig. 4.22.

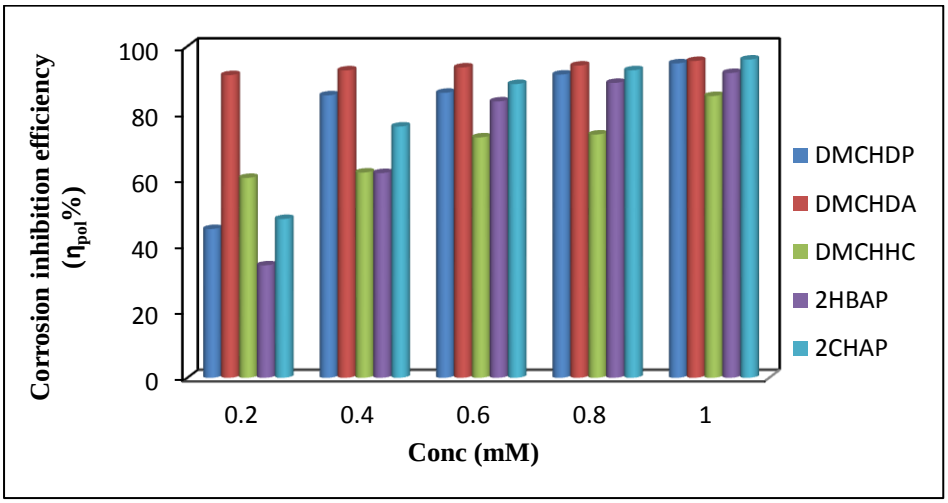

Fig. 4.22 Comparison of corrosion inhibition efficiency (η_{pol}%) of the Schiff bases on MS in 1.0 M HCl

Electrochemical noise measurements

Electrochemical noise measurements were carried out in a three-electrode system consisting of two mild steel electrodes having 1 cm^2 area and a saturated calomel electrode. The analysis was executed with the help of Ivium compactstat-e electrochemical system controlled by iviumsoft software. All electrochemical noise analyses were performed for a period of 1200s.

Current noise for MS in the absence and presence of Schiff bases (1 mM) in 1.0 M HCl are shown in Fig. 4.23. From the figure, it is clear that blank specimen exhibits higher mean value of current noise in respect of the specimen dipped in an acid medium containing Schiff base molecules. This reflects the high protective power of Schiff bases in 1.0 M HCl medium.

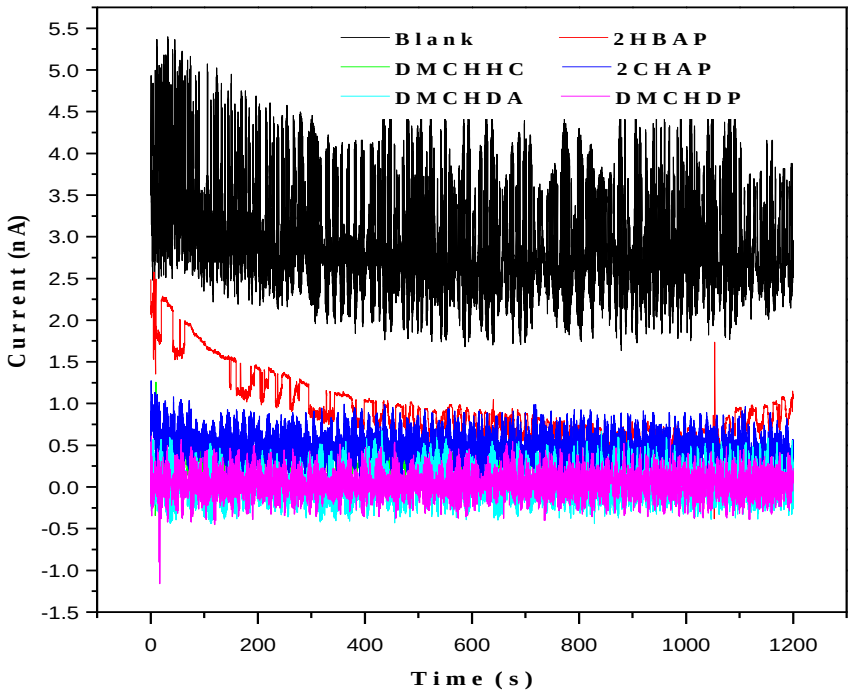

Fig. 4.23 Current noise for MS in the absence and presence of Schiff bases (1 mM) in 1.0 M HCl

Frequency domain analysis of noise measurement gave the PSD (power spectral density) plots of different systems, which is represented in Fig. 4.24. On detailed evaluation of PSD plots, it is evident that at all frequencies, the values of current noise are comparatively large for blank metal specimen than for metal immersed in acid solution containing Schiff base molecules. This suggests that localised corrosion of mild steel is occurring in acid solution without Schiff base molecule. Pitting index is a measure of resisting power to localised pitting corrosion. Pitting index curves are shown in Fig. 4.25. Amplitude of the pitting index curve corresponding to blank metal specimen is lower than metal specimens treated with acid solution containing Schiff base molecules. This implies that acid solution containing a Schiff base molecule has higher resistance to pitting corrosion.

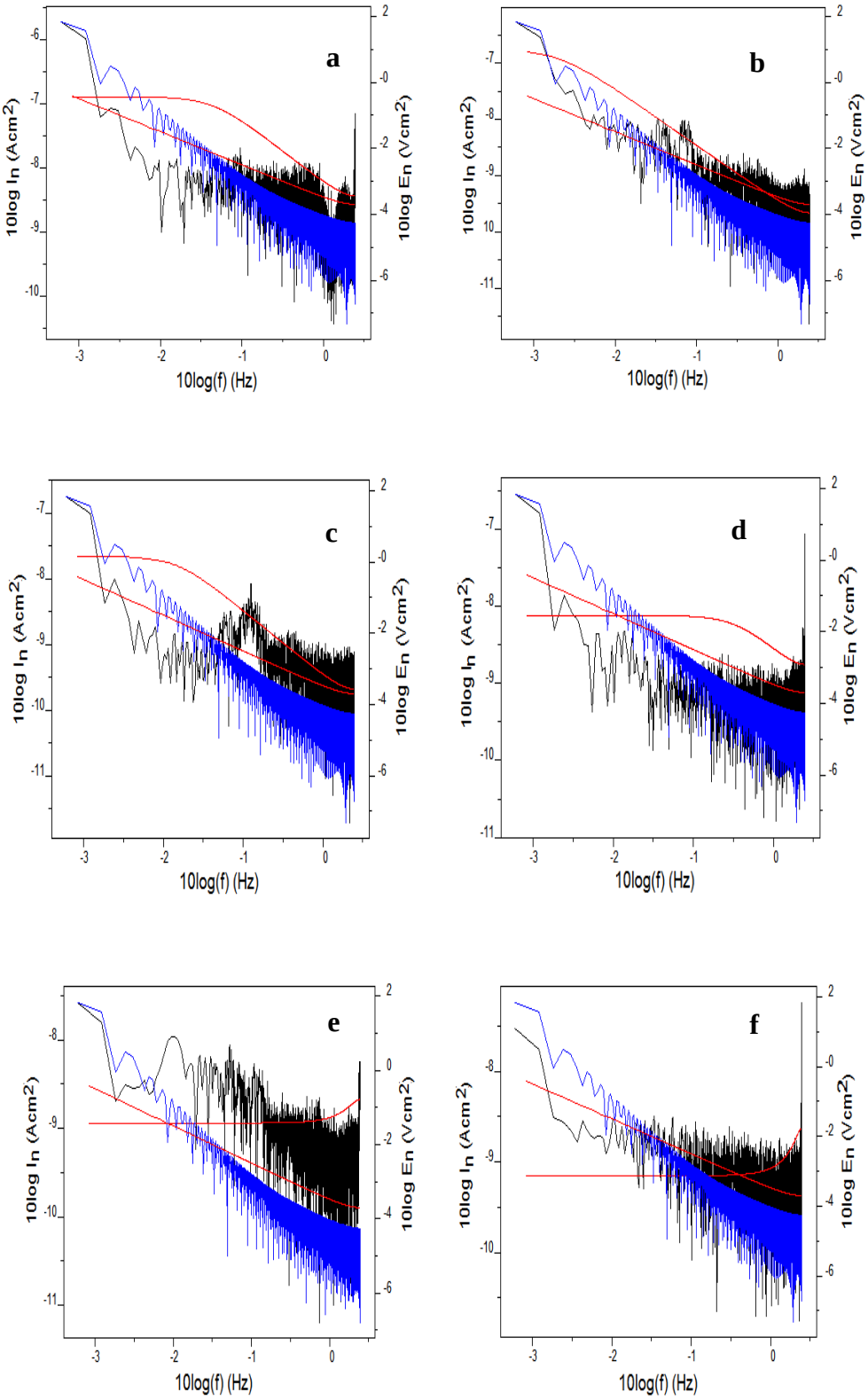

Fig. 4.24 Power spectral density (voltage and current) plots of MS in 1.0 M HCl in the presence a) blank b) 2HBAP c) DMCHHC d) 2CHAP e) DMCHDA and f) DMCHDP

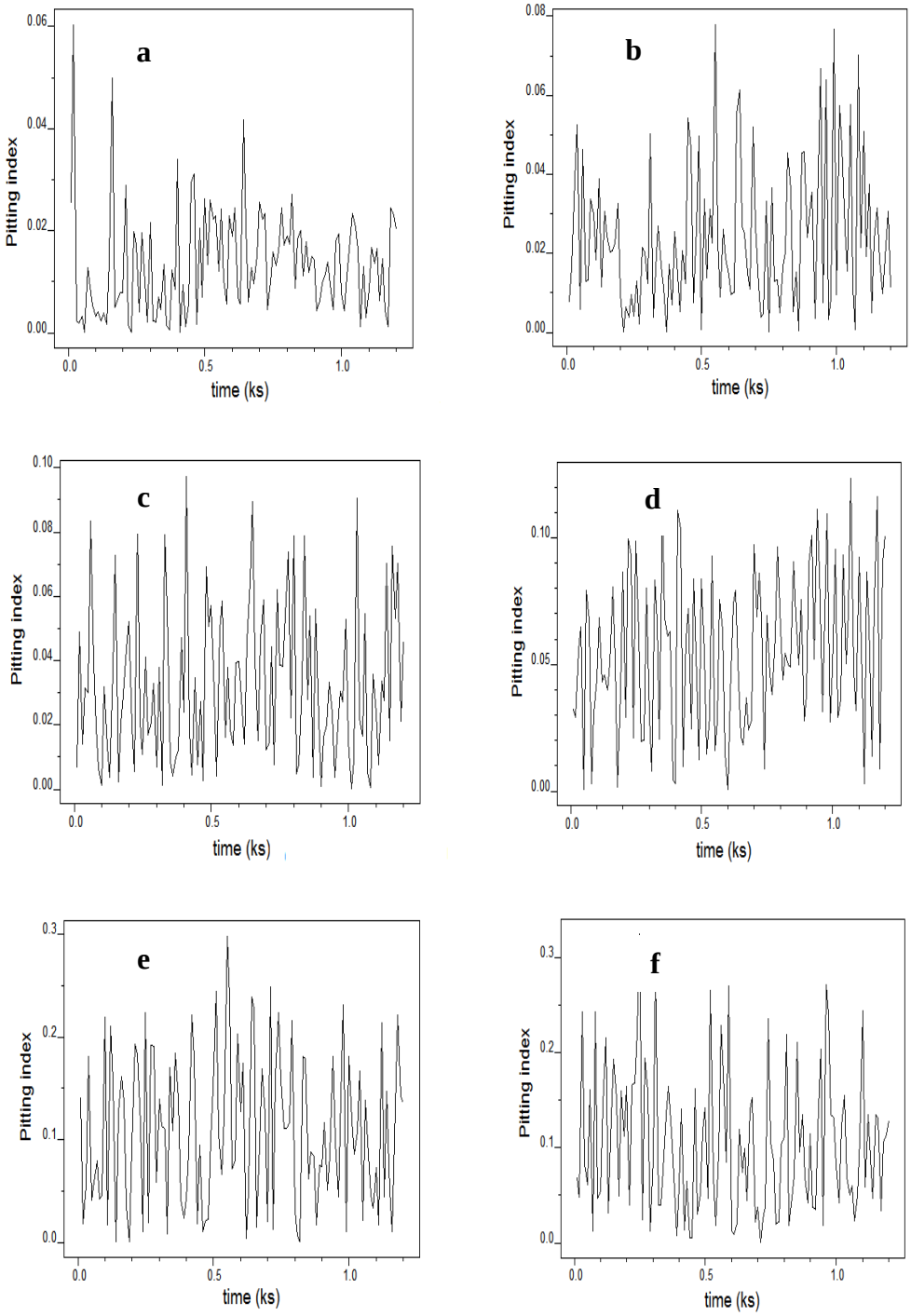

Fig. 4.25 Pitting index curve of MS in 1.0 M HCl in the presence a) blank b) 2HBAP c) DMCHHC d) 2CHAP e) DMCHDA and f) DMCHDP

Surface morphological studies

The surface morphological studies of the MS coupons were done by scanning electron microscope. Fig. 4.26(a-d) represents the SEM images of bare metal and in the

presence and absence of Schiff bases DMCHDP and DMCHDA (1.0 mM). Morphological studies clearly established that the surface of polished mild steel coupon before treatment in acid solution was smooth and not corroded as shown in Fig. 4.26a.

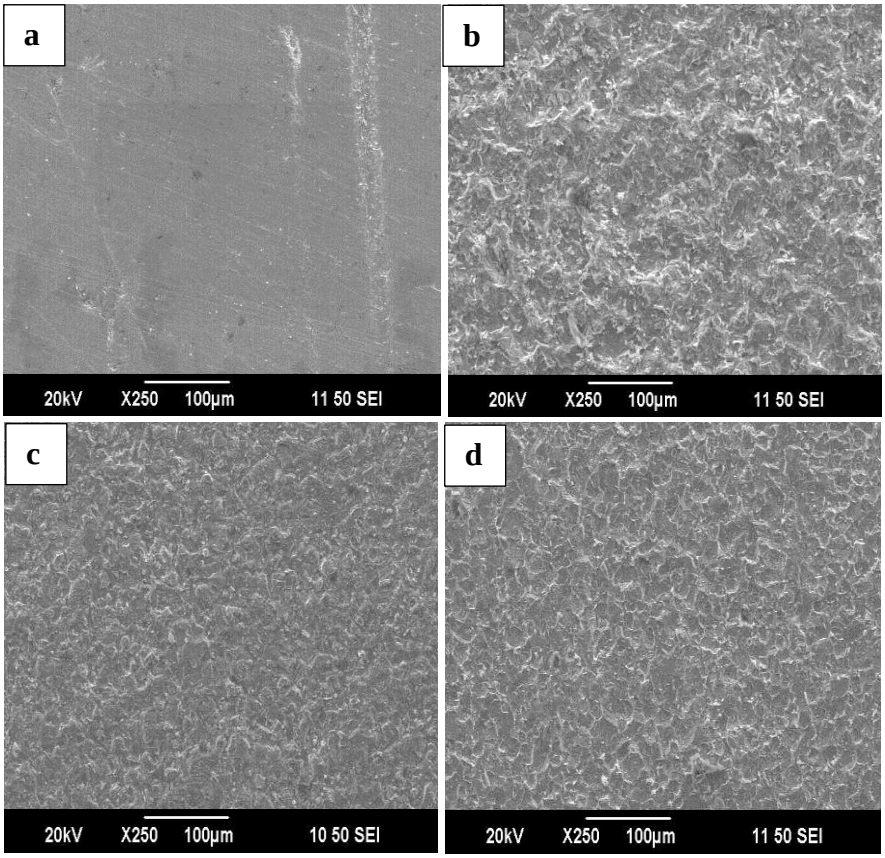

Fig. 4.26 SEM images of MS coupons before and after 24 h immersion a) bare b) blank (1.0 M HCl) c) treated with DMCHDP (1 mM) in 1.0 M HCl d) treated with DMCHDA (1 mM) in 1.0 M HCl

Significant change in the surface morphology was noticed after immersion in aggressive medium without Schiff bases (Fig. 4.26b). It is clear from the Fig. 4.26b, c and d that corrosion is more prominent in the case of MS coupon immersed in acid solution in the absence of Schiff bases. However in the presence of 1.0 mM concentration of DMCHDP and DMCHDA, rate of corrosion was decreased and the surface deterioration has been reduced (Fig. 4.26 c and d). This is due to the surface coverage of the Schiff bases molecule containing imine group. Aromatic rings and the azomethine linkage play great role in preventing dissolution of the metal and thereby protecting the mild steel from corrosion.

Quantum chemical investigations

Density functional theory (DFT) method is powerful theoretical tool for understanding the corrosion inhibition mechanism of organic molecules. There is a strong relationship between the energy gap of HOMO and LUMO with hardness and softness in accordance with HSAB concept. Inhibitor is defined as soft base when the energy gap between HOMO and LUMO is small and thus it have a tendency to coordinate with metals which are soft acid. Softness will increase when the corrosion inhibition tendency is high. In the electronic configuration $[Ar]4s^2 3d^6$ of Fe atom the 3d orbital is only partially filled. Thus this 3d orbital will bind with HOMO of the Schiff base molecule. Also the electrons in the filled 4s orbital are donated to LUMO of Schiff bases. Hence the Schiff base is adsorbed on the surface of the metal by the interaction of Fe atom orbital (4s and 3d) with HOMO and LUMO of Schiff bases. When the energy of LUMO decreases the energy gap will also decreases and as a result corrosion inhibition efficiency increases. In the present study the corrosion inhibition efficiency of five Schiff base ligands DMCHDP, DMCHDA, DMCHHC, 2HBAP and 2CHAP were evaluated using quantum chemical parameters. The values of parameters are shown in Table 4.9.

Table 4.9 Quantum chemical parameters of the Schiff base molecules calculated using DFT method

Schiff base	E_{HOMO} (eV)	E_{LUMO} (eV)	ΔE (eV)	χ (eV)	η (eV)	ΔN
DMCHDP	-1.7959	-0.1632	1.6327	0.9795	0.8163	3.687
DMCHDA	-1.6326	0.0544	1.6870	0.7891	0.8435	3.681
DMCHHC	-1.9047	-0.1904	1.7142	1.4075	0.8568	3.263
2HBAP	-3.2925	1.0612	4.3537	1.1156	2.1781	1.350
2CHAP	-3.0748	1.8503	4.9250	0.6122	2.4620	1.297

From the table it is clear that the energy gap between HOMO and LUMO is low in the case of DMCHDP, DMCHDA and DMCHHC on comparing with 2HBAP and 2CHAP. Thus the corrosion inhibition capacity of the ligands DMCHDP, DMCHDA and

DMCHHC will be high than the other two ligands. This result is in good agreement with that obtained from weight loss studies. Frontier molecular orbitals of the Schiff bases are shown in Fig. 4.27, 4.28, 4.29, 4.30 and 4.31. Optimized geometries of the Schiff bases are given in Fig 4.32.

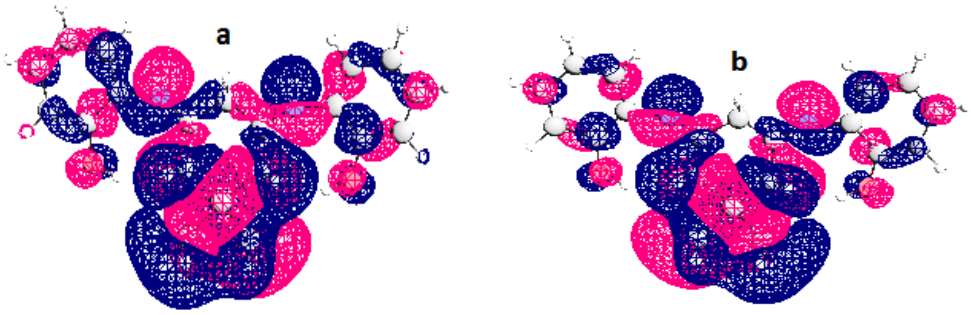

Fig. 4.27 Frontier molecular orbitals a) HOMO and b) LUMO of DMCHDP

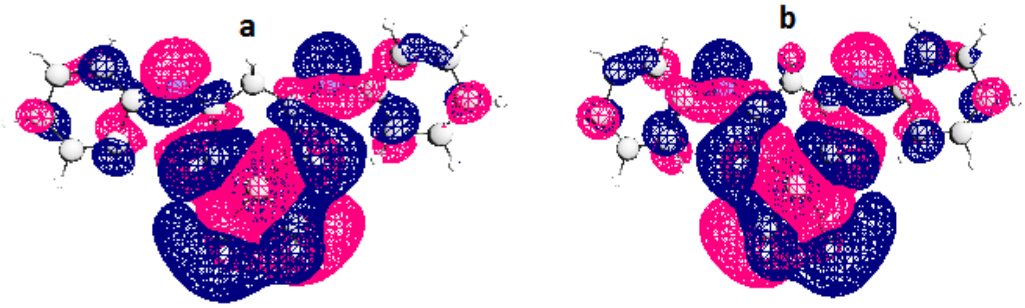

Fig. 4.28 Frontier molecular orbitals a) HOMO and b) LUMO of DMCHDA

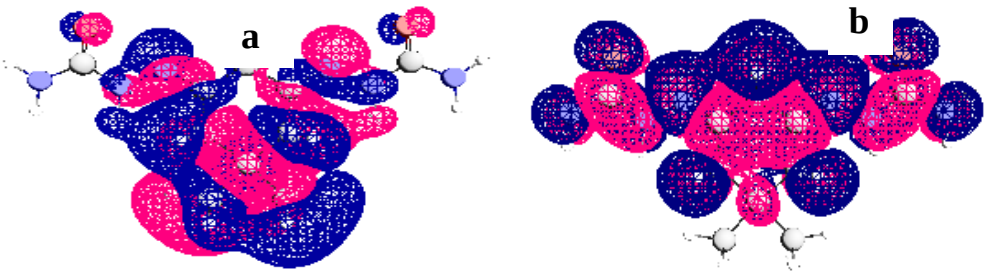

Fig. 4.29 Frontier molecular orbitals a) HOMO and b) LUMO of DMCHHC

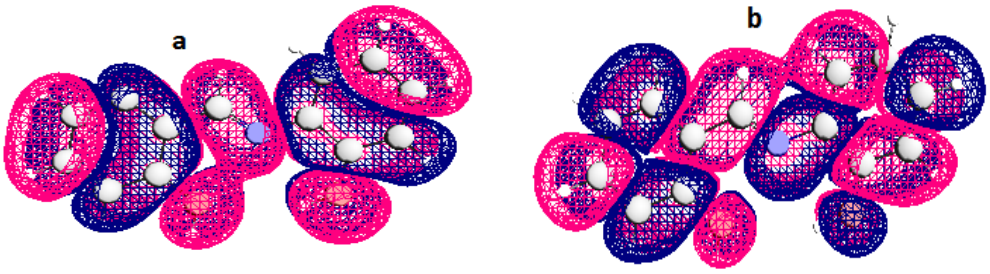

Fig. 4.30 Frontier molecular orbitals a) HOMO and b) LUMO of 2HBAP

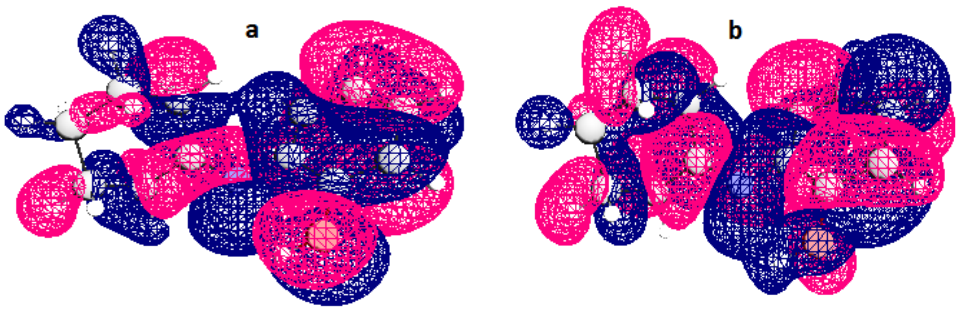

Fig. 4.31 Frontier molecular orbitals a) HOMO and b) LUMO of 2CHAP

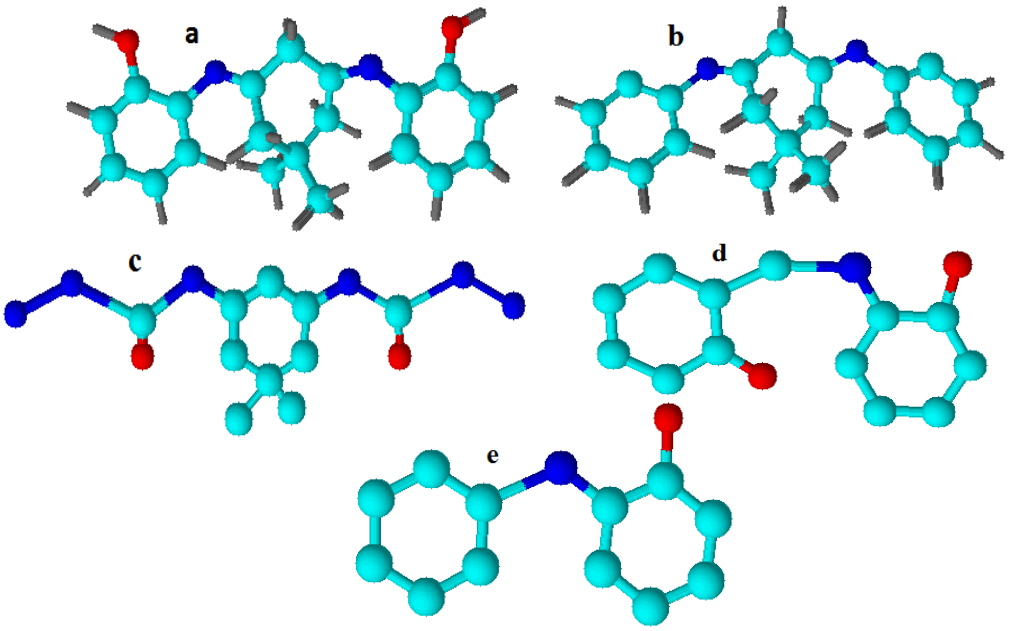

Fig. 4.32 Optimized geometries of the Schiff bases a) DMCHDP b) DMCHDA c) DMCHHC d) 2HBAP and e) 2CHAP